

## LETTER

**Rapid phytoplankton response to wind forcing influences productivity in upwelling bays**

Esperanza Broullón <sup>1\*</sup>, Peter J. S. Franks,<sup>2</sup> Bieito Fernández Castro <sup>3</sup>, Miguel Gilcoto <sup>4</sup>, Antonio Fuentes-Lema,<sup>1</sup> Maria Pérez-Lorenzo,<sup>1</sup> Emilio Fernández <sup>1</sup>, Beatriz Mouriño-Carballido <sup>1</sup>

<sup>1</sup>Centro de Investigación Mariña da Universidade de Vigo (CIM-UVigo), Vigo, Spain; <sup>2</sup>Scripps Institution of Oceanography, University of California San Diego, La Jolla, California; <sup>3</sup>Ocean and Earth Science, National Oceanography Centre, University of Southampton, Southampton, UK; <sup>4</sup>Departamento de Oceanografía, Instituto de Investigaciones Mariñas (IIM-CSIC), Vigo, Spain

**Scientific Significance Statement**

Coastal upwelling bays are ecological hotspots with exceptionally high productivity and fish catch. One unresolved question in these regions is why bays are more productive than shelf upwelled waters. Our study in two bays within the upwelling region off NW-Iberia, shows that the rapid response of phytoplankton growth to wind pulses inside the bays could explain their overall elevated biological productivity. The described mechanism underpinning the fast response may have implications for shellfish farming and the early detection of harmful algal blooms. Our results reveal that predictions of the evolution of coastal upwelling ecosystems under global change scenarios should consider not only trends in mean wind intensity, but also changes in the patterns of short-term wind variability.

**Abstract**

Bays are often ecological hotspots within highly-productive eastern boundary upwelling systems. Though the physics of such bays are well understood, there is no consensus about the factors underlying their high productivity. Three weeks of high-temporal-resolution observations in two long, narrow bays (Rías Baixas, NW-Iberia), showed that during an upwelling pulse, deep, nutrient-rich isopycnals rose into the euphotic zone inside the rías in a few hours. The response of the isopycnals to changes in wind forcing is approximately three times faster inside the rías than the Ekman spin-up time, triggering rapid nutrient uptake and subsequent formation of a subsurface chlorophyll and production maximum. The tight coupling and rapid response of phytoplankton growth to wind forcing could explain the higher productivity of the rías, and also be at play in other upwelling bays with similar morphologies and orientations. Resolving short-term variability of physical-biological coupling is crucial to discern the future evolution of upwelling bays.

\*Correspondence: [ebroullon@gmail.com](mailto:ebroullon@gmail.com)

**Associate editor:** Claudia Benitez-Nelson

**Author Contribution Statement:** EB, BFC, MG, and BM-C collected the data. AF-L and MP-L carried out the laboratory analysis. EB, BFC, and PF analyzed the data. EB, BFC, PF, EF, and BM-C prepared the manuscript with contributions from all the coauthors.

**Data Availability Statement:** Data and metadata are available at <https://doi.org/10.17632/pm4r2pyyh3.2>.

Additional Supporting Information may be found in the online version of this article.

This is an open access article under the terms of the [Creative Commons Attribution](https://creativecommons.org/licenses/by/4.0/) License, which permits use, distribution and reproduction in any medium, provided the original work is properly cited.

Eastern boundary upwelling systems (EBUS) are among the most productive ocean ecosystems, supporting 10% of oceanic new production (Fréon et al. 2009), despite covering only 1% of the global ocean's surface. As localized ecological hot-spots within EBUS, bays display a particularly rich suite of dynamical and ecosystem responses (Largier 2020), which have profound implications for the functioning of biological communities and the subsequent supply of ecosystem services. Bays are influenced by physical, chemical and biological processes driven by coastal upwelling in the adjacent ocean, but also by several local processes that can enhance the upwelling effect.

The extraordinary productivity of upwelling bays compared to offshore waters has been attributed to enhanced water column stratification, the intensity and persistence of upwelling conditions (GEOHAB 2005), as well as to longer retention times (Largier 2020) that allow phytoplankton extra time to assimilate nutrients. Moreover, nutrient availability in bays is enhanced by other sources in addition to upwelling of deep waters (Brown and Ozretich 2009), such as freshwater inputs (Barton et al. 2016), sediment-water column fluxes, or inputs associated with sewage (Fernández et al. 2016). Upwelling bays can also be nutrient-enriched through subsurface remineralization of organic matter produced in the bay and exported to the shelf during downwelling (Alvarez-Salgado et al. 1993). Despite these insights, the complexity of these systems makes it difficult to determine the actual processes driving the exceptional productivity of upwelling bays.

The Galician Rías Baixas are four long, narrow bays located at the northern limit of the Canary Current EBUS. Here, coastal upwelling supports a highly productive food chain and one of the most important blue economies in Europe (Figueiras et al. 2002; Garza-Gil et al. 2017). Due to their mid-latitude location, the upwelling dynamics are governed by synoptic-scale wind variability, which displays a strong seasonal modulation (Wooster et al. 1976). Southward, upwelling-favorable winds prevail between April and October, whereas northward, downwelling-favorable winds occur from October to March (Wooster et al. 1976). As a consequence of fluctuating synoptic forcing, upwelling in these bays is not a steady process with a large-scale equilibrium between the wind stress, the Coriolis force, and baroclinic pressure gradient, as in the classical formulations (Bowden 1983). Instead, upwelling occurs as a series of transient events with a typical duration of 3.3 d, interspersed with relaxation or downwelling events (Gilcoto et al. 2017). The circulation of the rías responds to changes in the wind forcing within 6 h, suggesting a barotropic, non-rotational spin-up of upwelling (Gilcoto et al. 2017). This is considerably faster than expected in a classical coastal upwelling system, where the shortest time scales are given by the rotational spin-up of the Ekman surface layer (Allen 1973): the inertial period (17.85 h at 42.23°N).

Previous studies in the region indicate that phytoplankton blooms are not steady but rather occur in pulses due to the variability in the wind forcing (Cermeño et al. 2006). The

coupling between turbulent mixing and phytoplankton growth has been studied in this system at seasonal and sub-seasonal time scales (Comesaña et al. 2021). However, the limited temporal resolution of these studies (1 week at best) has precluded a direct assessment of the effects of the short-term (3.3 d) transient upwelling events on phytoplankton growth, and their implications for the productivity of the ecosystem.

In order to discern the role of the short and rapid upwelling pulses in the productivity of these ecosystems, we investigated the coupling between upwelling pulses and phytoplankton growth using high temporal-spatial resolution data collected at the Rías Baixas during 3 weeks the summer of 2018. We sampled a grid of 84 stations comprising the Rías and adjacent shelf four times. These high-spatial-resolution samplings were interspersed with high-temporal-resolution observations at one specific station inside Ría de Pontevedra—a ría characterized by long harvesting closures due to detection of harmful toxins above regulatory levels (Broullón et al. 2020).

## Methods

The REMEDIOS-TLP cruise was carried out between 29 June and 16 July 2018 in the northwest of the Iberian Peninsula, specifically in two long, narrow bays (Ría de Pontevedra and Ría de Vigo), and the adjacent shelf (Fig. 1c). A grid of 84 stations throughout the area (Fig. S1) was sampled during four high-spatial-resolution surveys (“S”) on board of the R/V Ramón Margalef: S01 (29 June to 01 July), S02 (06–07 July), S03 (09–10 July), and S04 (14–16 July). The survey samplings were interspersed by three periods of intensive (“I”) high-temporal-resolution sampling at a fixed station inside the Ría de Pontevedra (Sta. 222, 30 m, 42.35°N, 8.77°W): I01 (02–06 July), I02 (07–09 July), and I03 (10–14 July).

During the high-spatial-resolution survey samplings (S01–S04), a SBE911 conductivity-temperature-depth (CTD) profile was acquired at each station. The SBE911 was equipped with fluorescence and photosynthetically active radiation sensors. A shelf station (333, 100 m, 42.30°N, 9.01°W) was sampled once during each survey to collect water at five depths for the determination of primary production. During the high-temporal-resolution intensive samplings (I01–I03), CTD profiles were acquired with a MSS90 microstructure profiler (Prandke and Stips 1998) equipped with, among other sensors, a fluorescence sensor. A set of five consecutive casts were performed every half hour, leaving < 15 min break between groups of five profiles, gathering a total of 1675 profiles over the three intensive sampling periods. These continuous measurements were paused every 6 h (08:00 h, 14:00 h, 20:00 h, 02:00 h) to conduct water collection at five to eight depths with a rosette equipped with 12 Niskin bottles, for determination of inorganic nutrients, chlorophyll *a* and primary production. Methods corresponding to the calibration of fluorescence sensors and the determination of primary production rates are included in the Text S1.2.

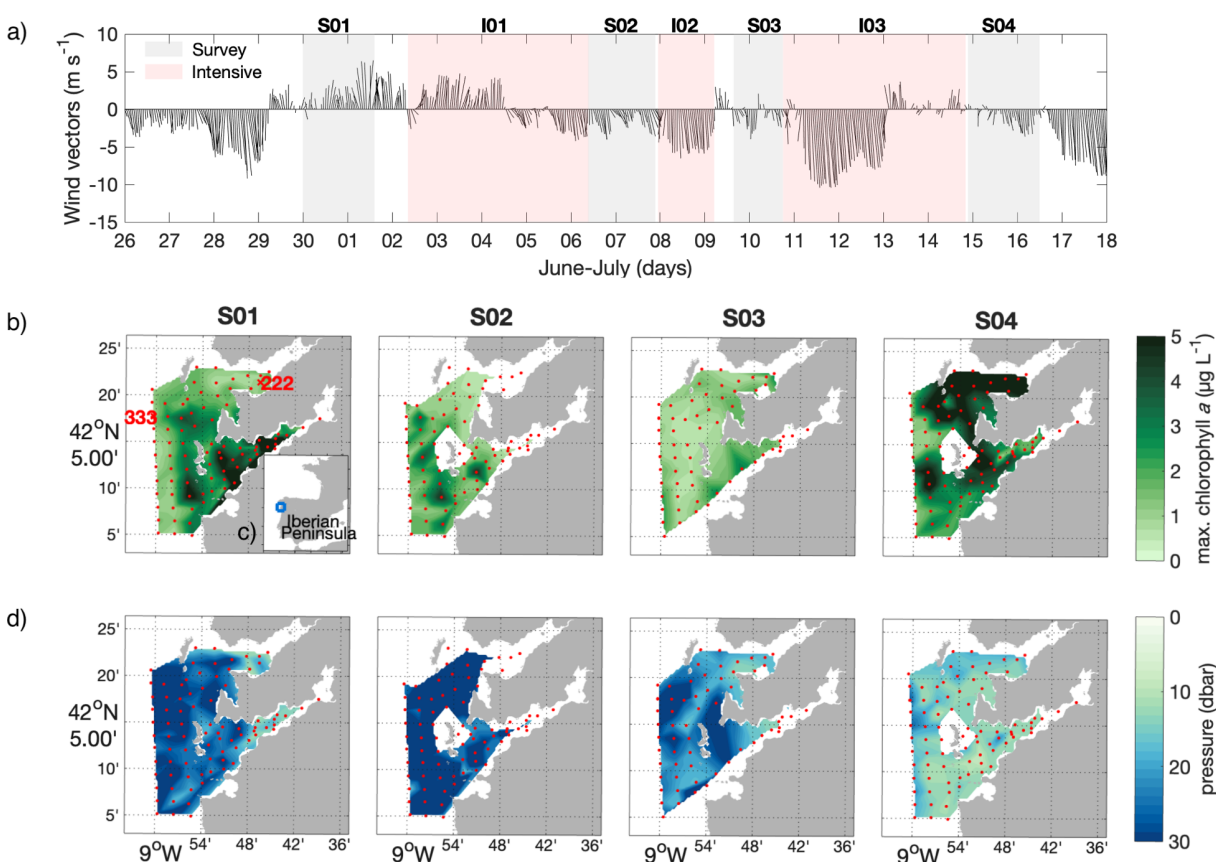


**Fig. 1.** (a) Time series of shelf wind vectors throughout the cruise. Negative (positive) values correspond to upwelling (downwelling) favorable winds, mainly southward (northward) winds. Gray shaded areas show the survey sampling periods S01–S04, whereas the red areas indicate the intensive samplings I01–I03. (b) Maximum chlorophyll *a* within the isopycnal range  $\sigma_\theta = 26.4\text{--}27 \text{ kg m}^{-3}$ . The first map shows the location of the intensive station, 222, and shelf station, 333. (c) Study area location within the Iberian Peninsula. (d) Pressure at the maximum chlorophyll *a* concentration, within the same isopycnal range as b. Red dots in b and d correspond to the stations sampled in each survey.

All data collected during the cruise are publicly available (Broullón et al. 2022).

A proxy for the depth of the euphotic zone was computed as the depth of 10% incident irradiance. The bottom depth of most stations inside the Rías ( $\sim 30 \text{ m}$ ) was shallower than the depth where the traditional value (1% incident irradiance) would be located, and most of the phytoplankton production occurred when the subsurface chlorophyll maximum was around the 10% isolume.

To determine nitrate concentrations, samples were frozen in situ at  $-18^\circ\text{C}$  and analyzed on land with a Skalar San Plus segmented flux analyzer. Primary production rates were determined by running incubations with the radioisotope  $^{14}\text{C}$ . The detailed methodology is described in Text S1.2.

Offshore wind data spanning the REMEDIOS-TLP period were acquired from an oceanographic buoy at the shelf ( $42.12^\circ\text{N}$ ,  $9.43^\circ\text{W}$ ; Fig. S1) operated by Puertos del Estado (data available at [www.puertos.es](http://www.puertos.es)); wind data near the intensive station were acquired from the meteorological station located at Cabo Udra, Bueu ( $42.34^\circ\text{N}$ ,  $8.82^\circ\text{W}$ ;

Fig. S1) operated by Meteogalicia (data available at [www.meteogalicia.gal](http://www.meteogalicia.gal)).

## Results

Time series of shelf wind (Fig. 1a) showed a strong upwelling-favorable wind event before the cruise, which relaxed a few hours before the initial high-spatial-resolution survey (S01). The following days were characterized mainly by northward, downwelling-favorable winds until the middle of the first high-temporal-resolution intensive sampling (I01), on 04 July. Subsequently, southward, upwelling-favorable winds increased to a maximum on 11–13 July, during I03. This increase was interrupted by 2 d of weak winds coinciding with S03, on 09–10 July. Finally, the last 3–4 d of the cruise, coinciding with S04, were dominated by upwelling relaxation.

The subsurface chlorophyll maximum tended to follow isopycnals and was located between  $\sigma_\theta = 26.4\text{--}27 \text{ kg m}^{-3}$  during the study (hereinafter chlorophyll-rich isopycnals) (Fig. 1b,d). During the field campaign, these isopycnals fluctuated up and

down, and in and out of the rías depending on the upwelling/relaxation/downwelling state.

The first spatial survey sampling, S01, was conducted a day after an upwelling event, and during a downwelling event. High mean maximum chlorophyll values of ( $2.6 \pm 1.9 \mu\text{g L}^{-1}$ ; concentration and standard deviation) were detected over the whole area (Fig. 1b). In Ría de Vigo and over the shelf, chlorophyll concentrations were  $> 5 \mu\text{g L}^{-1}$  at several stations. The mean depth of the chlorophyll-rich isopycnals was  $26 \pm 8$  m, deeper than the 10% isolume in the rías (mean depth  $16 \pm 2$  m), and deeper outside ( $> 20$  m) than inside the rías (18 m).

During S02, 2 d after a downwelling event, the chlorophyll maximum was weaker ( $1.5 \pm 1.0 \mu\text{g L}^{-1}$ ), and deeper ( $32 \pm 9$  m) than during S01. Moreover, the chlorophyll-rich isopycnal range was not present in the inner part of the rías, due to the downwelling winds.

The subsurface chlorophyll maximum was the weakest during S03 ( $1.2 \pm 0.6 \mu\text{g L}^{-1}$ ), but it was shoaling ( $23 \pm 7$  m in the rías) following upwelling-favorable conditions during the

preceding days. By survey S04, after a strong upwelling pulse, the chlorophyll-rich isopycnals were located much shallower than during previous surveys ( $15 \pm 4$  m in the rías), and reaching the highest concentrations ( $3.3 \pm 1.8 \mu\text{g L}^{-1}$ ).

The intensive samplings at a single station in the ría, I01–I03, offer a higher-temporal-resolution view of the chlorophyll fluctuations inside the rías in response to wind variability (Fig. 2b–d). In particular, the chlorophyll-rich isopycnals displayed large vertical excursions of up to 25 m (close to the full depth range), following the various upwelling–downwelling cycles. With the onset of downwelling-favorable winds at the beginning of I01, the chlorophyll-rich isopycnals (centered at  $26.55 \text{ kg m}^{-3}$ ) deepened ( $29 \pm 3$  m) and showed only weak chlorophyll values ( $1.0 \pm 0.3 \mu\text{g L}^{-1}$ ). Toward the end of I01, winds shifted to weakly upwelling-favorable and the  $26.55 \text{ kg m}^{-3}$  isopycnal shoaled (Fig. 2b). Nitrate levels were very low, exceeding  $1 \mu\text{mol L}^{-1}$  only below the chlorophyll maximum when those isopycnals were present (Fig. 2b–d). The next intensive sampling, I02, occurred after several days of weak upwelling winds. During I02, the chlorophyll-rich

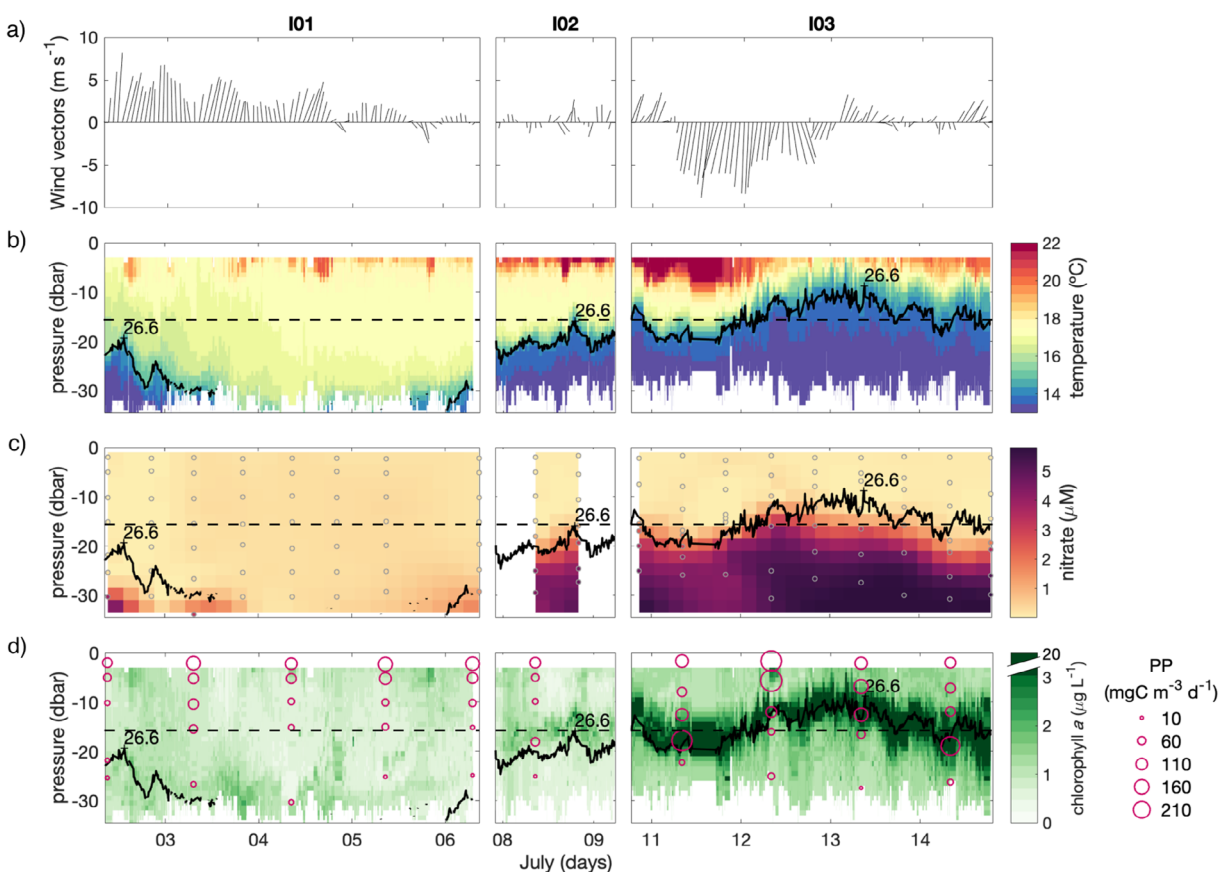


**Fig. 2.** Time-series of (a) local wind vectors. Negative (positive) values correspond to upwelling favorable (downwelling favorable) winds, mainly southward (northward) winds. (b) Temperature, (c) nitrate, and (d) chlorophyll *a* and primary production during the intensive sampling of Sta. 222 inside Ría de Pontevedra. Black solid lines in panels b, c, and d represent the  $26.6 \text{ kg m}^{-3}$  isopycnal. Black dashed lines in panels b, c, and d represent the mean 10% incident light at Sta. 222. Dots in panel c indicate when bottle samples were taken.

isopycnals shoaled, raising up to  $20 \pm 2$  m depth; maximum chlorophyll values were still low ( $0.8 \pm 0.3 \mu\text{g L}^{-1}$ ). During I03, after 2 d of relaxation when the chlorophyll-rich isopycnals deepened slightly, a period of sustained, intense upwelling caused the isopycnals to rapidly shoal further to  $< 10$  m, well within the euphotic zone. The shoaling isopycnals were accompanied by the upward movement of nutrient-rich water into the base of the euphotic zone (Fig. 2c). During this time the chlorophyll values increased to their highest values during the study ( $> 5 \mu\text{g L}^{-1}$ ).

Maximum primary production rates during I01 and I02 (mean value  $95 \pm 27 \text{ mgC m}^{-3} \text{ d}^{-1}$ ) were mainly located at the surface, and more than doubled during I03 ( $213 \pm 66 \text{ mgC m}^{-3} \text{ d}^{-1}$ ), when the highest rates were found in the chlorophyll-rich isopycnals. Mean depth-integrated values during I03 ( $2243 \pm 364 \text{ mgC m}^{-2} \text{ d}^{-1}$ ) were about threefold higher than depth-integrated values measured at the shelf (Sta. 333) during S03 and S04 ( $728 \pm 180 \text{ mgC m}^{-2} \text{ d}^{-1}$ ), 1 d before and after, respectively, the sampling conducted inside the ría during I03.

## Discussion

The different samplings undertaken during the cruise can be resorted in time to illustrate the response of the deep chlorophyll maximum to a typical wind-driven upwelling event (Fig. 3). Before the intensification of southward, upwelling-favorable winds, (as during I01 and S02), nutrient-rich isopycnals contain low chlorophyll values and are found relatively deep ( $> 30$  m) in waters over the shelf; they are not present in the shallow ( $< 25$  m) middle-inner part of the bays. When the wind starts blowing southwards (upwelling favorable), a circulation develops inside the rías driving the surface layer offshore, causing the deep isopycnals to rapidly shoal in the inner part of the rías. This shoaling brings deep, nutrient-rich water up to the base of the euphotic zone, allowing an increase of subsurface chlorophyll concentrations there, as in I02 and S03. During this intense upwelling in the rías, the same isopycnals are still deep at the mouth of the ría, and over the shelf. If the upwelling-favorable wind continues, the nutrient-rich isopycnals eventually advect upward into the euphotic zone over the shelf. At this point, the bloom is more intense and widespread, with highest chlorophyll values found inside the bays where the isopycnals are shallower and have been in the euphotic zone for longer (e.g., I03 and S04). Finally, the wind relaxes or reverses to downwelling-favorable, causing the dense, chlorophyll-rich isopycnals to deepen, while waters are advected back offshore in the subsurface flow from the rías. As the chlorophyll-rich layer deepens below the euphotic zone, the chlorophyll concentrations decrease at this layer, as found during S01.

The intensive sampling I03 illustrates the rapid biological response to wind-driven fluctuations of isopycnals in the ría. At the beginning of this sampling, at 18:00 h on 10 July, chlorophyll and primary production levels were high, but maximum

values were found at  $\sim 17$  m, due to the preceding upwelling/relaxation conditions (Fig. 3d). Upwelling-favorable winds started blowing at 04:00 h, on 11 July. Almost synchronously, the chlorophyll maximum layer reversed its deepening trend and began to shoal until 17:00 h on 12 July, remaining stable above 10 m for 21 h (Fig. 3c). The shoaling of the  $26.55 \text{ kg m}^{-3}$  isopycnal was associated with an immediate reduction of nitrate concentrations (Figs. 2c, 3b) and an increase in chlorophyll concentrations and primary production rates (Figs. 2d, 3c). This is consistent with the phytoplankton inhabiting these nutrient-rich isopycnals being exposed to light, and responding by rapidly taking up nutrients, with subsequent accumulation of biomass. This enhanced phytoplankton growth is restricted to the subsurface, nutrient-rich waters when they are exposed to light. The isolation of these isopycnals from the surface suggests that diapycnal mixing of nutrients into surface waters—a much slower process than the upward advection of isopycnals—plays a secondary role in the rapid development of the bloom.

The timescales of the phytoplankton response during I03 can be computed as the *e*-folding times of nitrate uptake ( $\tau_{\text{NO}_3^-} = 1.74 \text{ d}$ , Fig. 4a) and chlorophyll accumulation ( $\tau_p = 3.80 \text{ d}$ , Fig. 4b) calculated from temporal changes in the isopycnal range of the chlorophyll maximum. The wind decorrelation time scale of 3.2 d, which characterizes the duration of an upwelling event, was computed for the complete 2018 upwelling season (Fig. 4c), is consistent with previous estimates of the duration of a typical upwelling event (Gilcoto et al. 2017). The biological time scales are thus comparable to or shorter than the duration of an upwelling event, allowing the phytoplankton biomass to increase exponentially within this period.

This biophysical coupling is intensified by the rapid response of the vertical isopycnal displacement in the rías to changes in wind forcing—much faster than the Ekman spin-up time—which is underpinned by shape and dynamical characteristics of the bays. Local winds are funneled along the rías by the local topography, such that upwelling-favorable winds over the shelf occur synchronously with down-bay winds (Herrera et al. 2005; Gilcoto et al. 2017). Because the rías are relatively narrow and deep (deeper than the Ekman depth), the fast initial response to wind forcing occurs through an along-bay momentum balance involving the local wind stress, the barotropic pressure gradient, and friction (note: not Coriolis) (Lentz and Fewings 2012). This results in a rapid, linear spin-up of the exchange flow in response to upwelling/downwelling wind pulses (see Text S1.1). After the initial spin-up, the exchange flow is subsequently reinforced by the coupling of the slower rotational local (ría) and shelf responses (Souto et al. 2003; Barton et al. 2015; Gilcoto et al. 2017).

These rapid wind-driven fluctuations of the pycnocline may also occur in other wind-forced bays sharing the morphometric characteristics of the Galician Rías. However, many

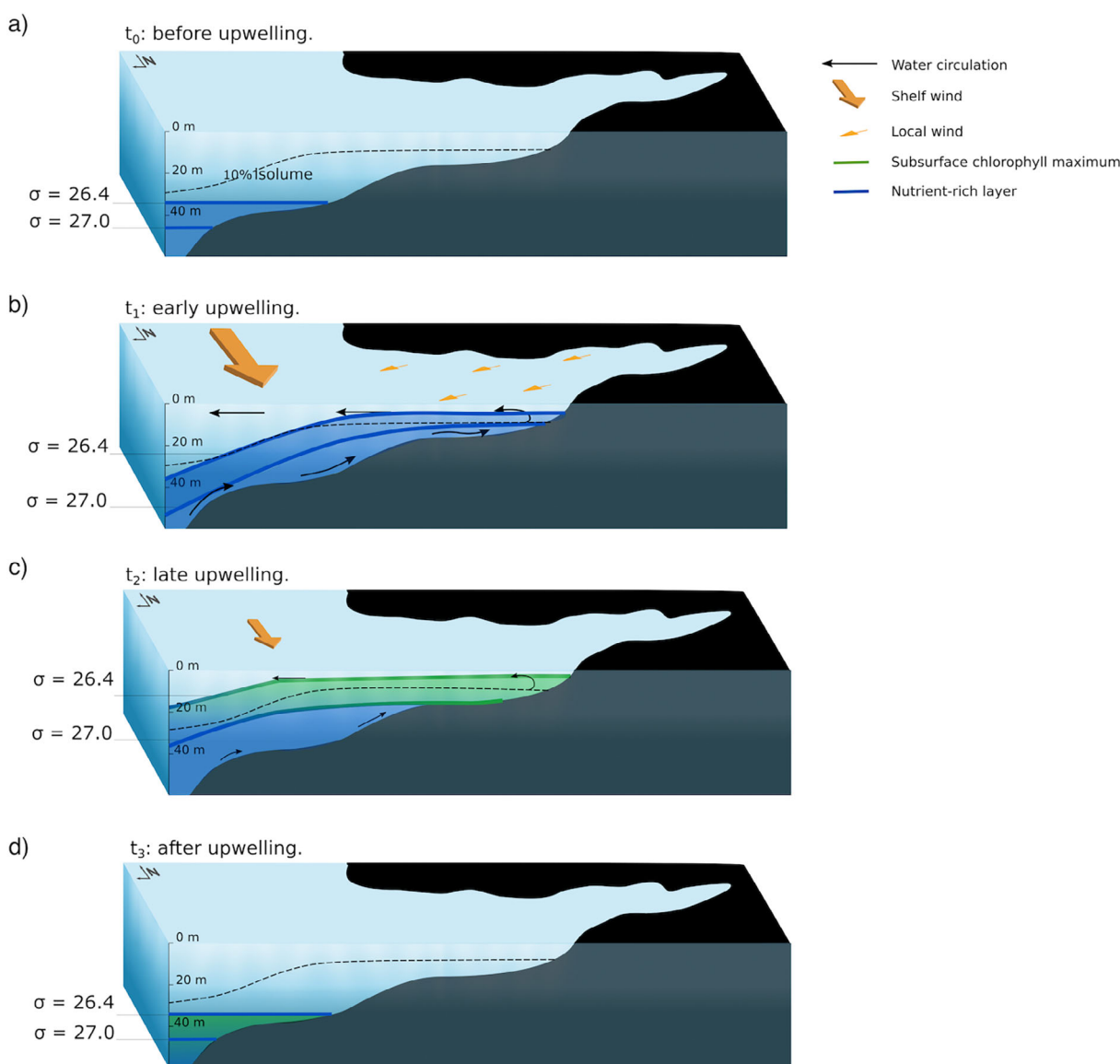


**Fig. 3.** 3D schematics of a wind-driven upwelling event in the studied bays. **(a)** Before upwelling: nutrient-rich isopycnals ( $\sigma_\theta = 26.4\text{--}27\text{ kg m}^{-3}$ ) are deep (I01 and S02) and absent from the bay. **(b)** Early upwelling: wind stress forces surface waters outside of the bay. In response, the isopycnals shoal into the euphotic zone inside the bay (I02 and S03). **(c)** Late upwelling: high chlorophyll biomass forms when the nutrient-rich isopycnals are raised into the euphotic zone over the whole area (I03 and S04). **(d)** After upwelling: as wind stops or reverses, the isopycnals deepen, carrying the high phytoplankton biomass downward and out of the bay (S01). Black dashed line represents the 10% isolume.

local factors (such as depth, length-width ratio, orientation or morphometry, among others) are responsible for the complex hydrodynamics of upwelling bays and their response to wind forcing. This fact makes it difficult to predict the timescale of the wind response by considering only their morphometry and orientation. The following is a series of upwelling bays, of great socioeconomic relevance, whose morphometry and orientation may allow to a rapid response to wind forcing, but not necessarily the only ones. Concepción Bay (Chile), located in the Humboldt EBUS, is also classified as an elongated bay (Largier 2020) and is oriented in the direction of

the wind field during upwelling (northward winds), but partially sheltered from upwelling transport due to its south-to-north alignment. Though data from Concepción Bay is not available, Peterson et al. (1988) and Daneri et al. (2012) studied Coliumo Bay, smaller but adjacent to Concepción Bay, and with a similar orientation, showing that transient upwelling events driven by synoptic wind forcing modulated the high primary productivity of this area (Daneri et al. 2012). Both studies showed a time lag between wind stress and hydrographic fluctuations of about 1 d, which is consistent with the local inertial period

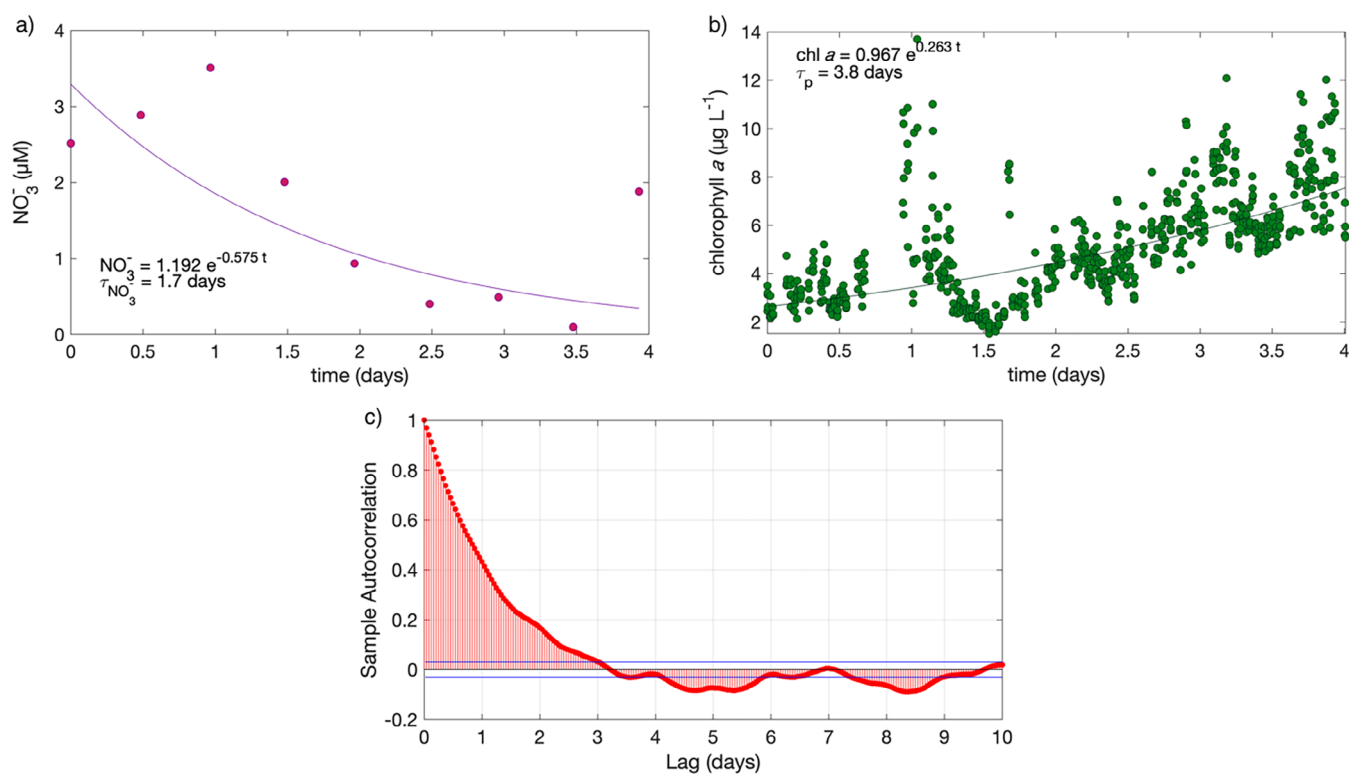


**Fig. 4.** Exponential fits of (a) nitrate and (b) chlorophyll vs. time at  $\sigma_0 = 26.4\text{--}27 \text{ kg m}^{-3}$  during I03. Fitted equations and e-folding times for chlorophyll ( $\tau_p$ ) and nitrate ( $\tau_{\text{NO}_3^-}$ ) are shown. (c) Ten days of the autocorrelation function and 95% confidence intervals (blue lines) for along-shore wind from the full 2018 upwelling season time series (15 April–15 October).

( $\sim 20 \text{ h}$ ); we would predict changes on an hourly time scale due to the similarity of this bay to our system. However, the low temporal resolution of these studies did not allow detection of rapid hydrographic fluctuations.

Another elongated bay, Dakhla Bay, located in the Canary Current EBUS (Largier 2020) is one of the most productive areas in Morocco in terms of shellfish farming (Zidane et al. 2008). It is also oriented NE to SW, as the Rías Baixas, and the typical winds in the region are mainly from north and north-east (Van Camp et al. 1991; Zidane et al. 2008). This bay fits all the requirements to have rapid fluctuations of the subsurface chlorophyll maximum in response to both local and shelf wind forcing. However, no high-temporal-resolution samplings have been reported so far in this system.

The coupling between the time scales of wind forcing and phytoplankton growth helps to explain the higher phytoplankton productivity of the rías, and other similar upwelling bays, compared to offshore waters (Lorenzo et al. 2005; Arístegui et al. 2009). In our case, depth-integrated primary production rates were three times greater inside the ría, supporting this hypothesized mechanism. The succession of synoptic-scale upwelling events creates a highly perturbed scenario that favors phytoplankton functional groups such as diatoms (Cermeño et al. 2011), characterized by high maximum nutrient uptake and growth rates (Sommer 1984; Litchman 2007). The

mechanism presented in this study ensures that high mean primary productivity is maintained throughout the summer season, despite the flushing of biomass offshore after the cessation of upwelling-favorable winds (Piedracoba et al. 2005).

Our results have also implications for mussel farming, the most productive marine aquaculture activity in the region (Labarta and Fernández-Reiriz 2019). Mussels are cultured on 12-m long ropes hanging from rafts. The intermittent presence of nutrient- and food-rich water near the surface during upwelling is likely to affect mussel food supply and growth. Local mussel farmers report that, while mussels located near the surface grow about twice as fast as mussels deeper down on the ropes, mussels at the deepest end of the rope (10–12 m) were often much larger than mussels at intermediate depths. These mussels are likely accessing the subsurface nutrient-rich, high-chlorophyll layer. It is possible that longer ropes—with more frequent access to this layer—could benefit the mussel culture. Our results could also have implications for the early detection of harmful algal blooms, as the chlorophyll maximum going in and out the ría could seed the ría with harmful algae (Seegers et al. 2015); such short-term, small-scale patches could be easily missed by monitoring programs at fixed stations inside the bays.

Productivity in upwelling ecosystems is traditionally linked to upwelling intensity and duration, both expected to increase

at high latitudes and decrease at low latitudes under global change scenarios (Fox-Kemper et al. 2021). However, our study reveals that the resonance between the time scales of wind-driven upwelling pulses ( $\sim 3$  d) and phytoplankton growth could drive the higher phytoplankton productivity observed in long, narrow upwelling bays. Therefore, highly spatially and temporally resolved surveys, such as those presented in this study, are crucial for discerning the specific drivers of primary production of upwelling bays, and their evolution under different global change scenarios.

## References

- Allen, J. S. 1973. Upwelling and coastal jets in a continuously Stratified Ocean. *J. Phys. Oceanogr.* **3**: 245–257. doi:10.1175/1520-0485(1973)003<0245:uacjia>2.0.co;2
- Alvarez-Salgado, X. A., G. Rosón, F. F. Pérez, and Y. Pazos. 1993. Hydrographic variability off the Rías Baixas (NW Spain) during the upwelling season. *J. Geophys. Res.: Oceans* **98**: 14447–14455. doi:10.1029/93jc00458
- Aristegui, J., and others. 2009. Sub-regional ecosystem variability in the canary current upwelling. *Prog. Oceanogr.* **83**: 33–48. doi:10.1016/j.pocean.2009.07.031
- Barton, E. D., J. L. Largier, R. Torres, M. Sheridan, A. Trasviña, A. Souza, Y. Pazos, and A. Valle-Levinson. 2015. Coastal upwelling and downwelling forcing of circulation in a semi-enclosed bay: Ria de Vigo. *Prog. Oceanogr.* **134**: 173–189. doi:10.1016/j.POCEAN.2015.01.014
- Barton, E. D., R. Torres, F. G. Figueiras, M. Gilcoto, and J. Largier. 2016. Surface water subduction during a downwelling event in a semienclosed bay. *J. Geophys. Res.: Oceans* **121**: 7088–7107. doi:10.1002/2016JC011950
- Bowden, K. F. 1983, *Physical oceanography of coastal waters*. Ellis Horwood.
- Broullón, E., and others. 2020. Thin layers of phytoplankton and harmful algae events in a coastal upwelling system. *Prog. Oceanogr.* **189**: 102449. doi:10.1016/J.POCEAN.2020.102449
- Broullón, E., P. J. Franks, B. Fernández-Castro, M. Gilcoto, A. Fuentes-Lema, B. Mouriño-Carballido, M. Pérez, and E. Fernandez. 2022. Rapid fluctuations of the subsurface chlorophyll maximum in response to wind forcing in a long, Narrow Bay - Supplementary Information. Mendeley Data. 10.17632/PM4R2PYHH3.2
- Brown, C. A., and R. J. Ozretich. 2009. Coupling between the Coastal Ocean and Yaquina Bay, Oregon: Importance of oceanic inputs relative to other nitrogen sources. *Estuaries Coasts* **32**: 219–237. doi:10.1007/s12237-008-9128-6
- Cermeño, P., E. Marañón, V. Pérez, P. Serret, E. Fernández, and C. G. Castro. 2006. Phytoplankton size structure and primary production in a highly dynamic coastal ecosystem (Ría de Vigo, NW-Spain): Seasonal and short-time scale variability. *Coast. Shelf Sci.* **67**: 251–266. doi:10.1016/j.ecss.2005.11.027
- Cermeño, P., J. Lee, K. Wyman, O. Schofield, and P. Falkowski. 2011. Competitive dynamics in two species of marine phytoplankton under non-equilibrium conditions. *Mar. Ecol. Prog. Ser.* **429**: 19–28. doi:10.3354/meps09088
- Comesaña, A., B. Fernández-Castro, P. Chouciño, E. Fernández, A. Fuentes-Lema, M. Gilcoto, M. Pérez-Lorenzo, and B. Mouriño-Carballido. 2021. Mixing and phytoplankton growth in an upwelling system. *Front. Mar. Sci.* **8**: 712342. doi:10.3389/fmars.2021.712342
- Daneri, G., L. Lizárraga, P. Montero, H. E. González, and F. J. Tapia. 2012. Wind forcing and short-term variability of phytoplankton and heterotrophic bacterioplankton in the coastal zone of the Concepción upwelling system (Central Chile). *Prog. Oceanogr.* **92–95**: 92–96. doi:10.1016/J.POCEAN.2011.07.013
- Fernández, E., X. A. Álvarez-Salgado, R. Beiras, A. Ovejero, and G. Méndez. 2016. Coexistence of urban uses and shellfish production in an upwelling-driven, highly productive marine environment: The case of the Ría de Vigo (Galicia, Spain). *Reg. Stud. Mar. Sci.* **8**: 362–370. doi:10.1016/J.RSMA.2016.04.002
- Figueiras, F. G., U. Labarta, and M. J. F. Reiriz. 2002. Coastal upwelling, primary production and mussel growth in the Rías Baixas of Galicia, p. 121–131. In O. Vadstein and Y. Olsen [eds.], *Sustainable increase of marine harvesting: Fundamental mechanisms and new concepts*. Springer. doi:10.1007/978-94-017-3190-4\_11
- Fox-Kemper, B., and others. 2021. Ocean, cryosphere and sea level change. *Climate Change 2021 IPCC Sixth Assessment Report Working Group 1: The Physical Science Basis*. 1–257.
- Fréon, P., M. Barange, and J. Aristegui. 2009. Eastern boundary upwelling ecosystems: Integrative and comparative approaches. *Prog. Oceanogr.* **83**: 1–14. doi:10.1016/j.pocean.2009.08.001
- Garza-Gil, M. D., J. C. Surís-Regueiro, and M. M. Varela-Lafuente. 2017. Using input–output methods to assess the effects of fishing and aquaculture on a regional economy: The case of Galicia, Spain. *Mar. Policy* **85**: 48–53. doi:10.1016/J.MARPOL.2017.08.003
- GEOHAB. 2005. In G. C. Pitcher, M. T. Moita, V. L. Trainer, R. M. Kudela, F. G. Figueiras, and T. A. Probyn [eds.], *Global Ecology and Oceanography of Harmful Algal Blooms, GEOHAB Core Resesarch project*. IOC and SCOR.
- Gilcoto, M., and others. 2017. Rapid response to coastal upwelling in a semienclosed bay. *Geophys. Res. Lett.* **44**: 2388–2397. doi:10.1002/2016GL072416
- Herrera, J. L., S. Piedracoba, R. A. Varela, and G. Rosón. 2005. Spatial analysis of the wind field on the western coast of Galicia (NW Spain) from in situ measurements. *Cont. Shelf Res.* **25**: 1728–1748. doi:10.1016/j.csr.2005.06.001
- Labarta, U., and M. J. Fernández-Reiriz. 2019. The Galician mussel industry: Innovation and changes in the last forty

- years. *Ocean Coast. Manag.* **167**: 208–218. doi:[10.1016/j.ocecoaman.2018.10.012](https://doi.org/10.1016/j.ocecoaman.2018.10.012)
- Largier, J. L. 2020. Upwelling bays: How coastal upwelling controls circulation, habitat, and productivity in bays. *Ann. Rev. Mar. Sci.* **12**: 415–447. doi:[10.1146/annurev-marine-010419-011020](https://doi.org/10.1146/annurev-marine-010419-011020)
- Lentz, S. J., and M. R. Fewings. 2012. The wind- and wave-driven inner-shelf circulation. *Ann. Rev. Mar. Sci.* **4**: 317–343. doi:[10.1146/annurev-marine-120709-142745](https://doi.org/10.1146/annurev-marine-120709-142745)
- Litchman, E. 2007. Resource competition and the ecological success of phytoplankton, p. 351–375. In P. G. Falkowski and A. H. Knoll [eds.], *Evolution of primary producers in the sea*. Academic Press. doi:[10.1016/B978-012370518-1/50017-5](https://doi.org/10.1016/B978-012370518-1/50017-5)
- Lorenzo, L. M., B. Arbones, G. H. Tilstone, and F. G. Figueiras. 2005. Across-shelf variability of phytoplankton composition, photosynthetic parameters and primary production in the NW Iberian upwelling system. *J. Mar. Syst.* **54**: 157–173. doi:[10.1016/J.JMARSYS.2004.07.010](https://doi.org/10.1016/J.JMARSYS.2004.07.010)
- Peterson, W. T., D. F. Arcos, G. B. McManus, H. Dam, D. Bellantoni, T. Johnson, and P. Tiselius. 1988. The near-shore zone during coastal upwelling: Daily variability and coupling between primary and secondary production off Central Chile. *Prog. Oceanogr.* **20**: 1–40. doi:[10.1016/0079-6611\(88\)90052-3](https://doi.org/10.1016/0079-6611(88)90052-3)
- Piedracoba, S., X. A. Álvarez-Salgado, G. Rosón, and J. L. Herrera. 2005. Short-timescale thermohaline variability and residual circulation in the central segment of the coastal upwelling system of the Ría de Vigo (northwest Spain) during four contrasting periods. *J. Geophys. Res.: Oceans* **110**: C03018. doi:[10.1029/2004JC002556](https://doi.org/10.1029/2004JC002556)
- Prandke, H., and A. Stips. 1998. Test measurements with an operational microstructure-turbulence profiler: Detection limit of dissipation rates. *Aquat. Sci.* **60**: 191. doi:[10.1007/s000270050036](https://doi.org/10.1007/s000270050036)
- Seegers, B. N., and others. 2015. Subsurface seeding of surface harmful algal blooms observed through the integration of autonomous gliders, moored environmental sample processors, and satellite remote sensing in southern California. *Limnol. Oceanogr.* **60**: 754–764. doi:[10.1002/lno.10082](https://doi.org/10.1002/lno.10082)
- Sommer, U. 1984. The paradox of the plankton: Fluctuations of phosphorus availability maintain diversity of phytoplankton in flow-through cultures. *Limnol. Oceanogr.* **29**: 633–636. doi:[10.4319/lo.1984.29.3.0633](https://doi.org/10.4319/lo.1984.29.3.0633)
- Souto, C., M. Gilcoto, L. Farina-Busto, and F. F. Pérez. 2003. Modeling the residual circulation of a coastal embayment affected by wind-driven upwelling: Circulation of the Ría de Vigo (NW Spain). *J. Geophys. Res.: Oceans* **108**: 3340. doi:[10.1029/2002jc001512](https://doi.org/10.1029/2002jc001512)
- Van Camp, L., L. Nykjaer, E. Mittelstaedt, and P. Schlittenhardt. 1991. Upwelling and boundary circulation off Northwest Africa as depicted by infrared and visible satellite observations. *Prog. Oceanogr.* **26**: 357–402. doi:[10.1016/0079-6611\(91\)90012-B](https://doi.org/10.1016/0079-6611(91)90012-B)
- Wooster, W. S., A. Bakun, and D. R. McLain. 1976. The seasonal upwelling cycle along the eastern boundary of the North Atlantic. *J. Mar. Res.* **34**: 131–141.
- Zidane, H., A. Orbi, A. Mouradi, F. Zidane, and J.-F. Blais. 2008. Structure hydrologique et edaphique d'un site ostreicole: duna Blanca (La baie de Dakhla Sud du Maroc). *Environ. Technol.* **29**: 1031–1042. doi:[10.1080/09593330802180328](https://doi.org/10.1080/09593330802180328)

#### Acknowledgments

The authors would like to thank the captain, crew, and technicians of R/V Ramón Margalef as well as Nicolás Villacieros, Fernando Alonso, and Waldo Redondo from IIM-CSIC and Paloma Chouciño from Universidade de Vigo for their help in processing data from land during the REMEDIOS-TLP cruise and in the preparation of the equipment before. This research was funded by project REMEDIOS (CTM2016-75451-C2-1-R) to BM-C from the Spanish Ministry of Economy and Competitiveness. E.B. acknowledges a predoctoral fellowship (ED481A-2019/288) from Xunta de Galicia, cofunded by FSE Galicia (2014–2020). BFC was supported by the Spanish Ministry of Economy and Innovation through a Juan de la Cierva-Formación postdoctoral fellowship (grant number FJCI-641 2015-25712) and by the European Union's Horizon 2020 research and innovation program under the Marie Skłodowska-Curie grant agreement No. 834330 (SO-CUP). Bathymetry data used in the Fig. S1 was obtained from GEBCO Compilation Group 2020 (<https://doi.org/10.5285/a29c5465-b138-234d-e053-6c86abc040b9>).

Submitted 19 July 2022

Revised 16 December 2022

Accepted 22 December 2022